Atmos. Chem. Phys. Discuss., 10, 25355–25388, 2010
www.atmos-chem-phys-discuss.net/10/25355/2010/
doi:10.5194/acpd-10-25355-2010

Atmospheric Chemistry and Physics Discussions

Estimate of bias in Aura TES HDO/H_2O profiles from comparison of TES and in situ HDO/H_2O measurements at the Mauna Loa Observatory

J. Worden[1], D. Noone[2], J. Galewsky[3], A. Bailey[2], K. Bowman[1], D. Brown[2], J. Hurley[3], S. Kulawik[1], J. Lee[1], and M. Strong[3]

[1]Jet Propulsion Laboratory/California Institute of Technology, Pasadena, CA, USA
[2]University of Colorado, Boulder, CO, USA
[3]University of New Mexico, Albuquerque, NM, USA

Received: 4 October 2010 – Accepted: 15 October 2010 – Published: 1 November 2010

Correspondence to: J. Worden (john.worden@jpl.nasa.gov)

Published by Copernicus Publications on behalf of the European Geosciences Union.

Abstract

The Aura satellite Tropospheric Emission Spectrometer (TES) instrument is capable of measuring the HDO/H_2O ratio in the lower troposphere using thermal infrared radiances between 1200 and 1350 cm^{-1}. However, direct validation of these measurements is challenging due to a lack of in situ measured vertical profiles of the HDO/H_2O ratio that are spatially and temporally co-located with the TES observations. From 11 October through 5 November 2008, we undertook a campaign to measure HDO and H_2O at the Mauna Loa observatory in Hawaii for comparison with TES observations. The Mauna Loa observatory is situated at 3.1 km above sea level or approximately 680 hPa, which is approximately the altitude where the TES HDO/H_2O observations show the most sensitivity. Another advantage of comparing in situ data from this site to estimates derived from thermal IR radiances is that the volcanic rock is heated by sunlight during the day, thus providing significant thermal contrast between the surface and atmosphere; this thermal contrast increases the sensitivity to near surface estimates of tropospheric trace gases. The objective of this inter-comparison is to better characterize a bias in the TES HDO data, which had been previously estimated to be approximately 5% too high for a column integrated value between 850 hPa and 500 hPa. We estimate that the TES HDO profiles should be corrected downwards by approximately 4.1% and 5.6% for Versions 3 and 4 of the data, respectively. These corrections must account for the vertical sensitivity of the TES HDO estimates. We estimate that the uncertainty of this bias correction is approximately 1%. However, future comparisons of TES data to other sensors are needed to refine this bias estimate because these uncertainties are primarily derived from only three sets of measurements.

1 Introduction

Measurements of the isotopic composition of water vapor are useful for understanding the distribution of sources, sinks, and processes affecting water because the isotopic

ACPD
10, 25355–25388, 2010

composition of water vapor is sensitive to phase changes and also to the isotopic ratio, or "fingerprint", of the original moisture source (e.g., Craig, 1961; Dansgaard, 1964). Satellite measurements of the isotopic composition of water vapor have provided insights into the sources of water into the upper troposphere and lower stratosphere (e.g., Moyer et al., 1996; Kuang et al., 2003; Nassar et al., 2007; Payne et al. 2007; Steinwagner et al., 2010) and more recently for characterizing the distribution of hydrological processes in the free troposphere (e.g., Zakharov et al., 2004; Herbin et al., 2009; Worden et al., 2006, 2007; Brown et al., 2008; Frankenberg et al., 2009; Galewsky et al., 2007).

However, very few direct validations of these satellite measurements exist because of the difficulty in obtaining vertical profiles of the isotopic composition of water vapor that are co-located with satellite data. Most validations of these data have therefore relied on indirect comparisons of the distributions of water vapor isotopes between satellite and aircraft (e.g., Webster and Heymsfield, 2003) or validation of the H_2O measurements, which in turn can be used to assess the errors on the estimate of the HDO/H_2O ratio (e.g., Worden et al., 2006; Herbin et al., 2007, 2009). There are several currently operational sounders measuring the isotopic composition of water vapor such as the Tropospheric Emission Spectrometer (TES), the Atmospheric Chemistry Experiment (ACE), the Infrared Atmospheric Sounding Interferometer (IASI), the SCanning Imaging Absorption SpectroMeter for Atmospheric CHartographY (SCIAMACHY), and the Greenhouse gases Observing SATellite (GOSAT), as well as several future satellites such as the IASI 2 and the Tropospheric Ozone Monitoring Instrument (TropOMI, http://www.knmi.nl/samenw/tropomi/) that plan on measuring the isotopic composition of water vapor. In addition, the application of these measurements for assessing tropospheric and stratospheric moisture sources (evaporation), sinks (rain), cloud processes, and mixing processes is rapidly growing (e.g., Worden et al., 2007; Brown et al., 2008; Risi et al., 2008; Frankenberg et al., 2009; Lee et al., 2009; Galewsky et al., 2007). As a consequence there is a need for more robustly assessing the biases as well as the theoretical versus random errors in these data (e.g., Boxe et al., 2010),

ACPD
10, 25355–25388, 2010

especially for the lower tropospheric/boundary layer measurements where random errors in the satellite data can be as large or larger than the variability observed in the HDO/H_2O ratio using in situ measurements (e.g., Frankenberg et al., 2009).

Two new approaches for validation of satellite based tropospheric measurements of water vapor and its isotopes are now available. One relies on upward looking solar occultation measurements that can estimate vertical profiles of HDO and H_2O with approximately 1.5–2 degrees-of-freedom for signal (DOFS) (Schneider et al., 2006; Frankenberg et al., 2009); we do not use this approach in this study as it requires a targeted set of measurements from the TES satellite that have yet to be implemented. In this paper we describe the results of an inter-comparison campaign from 8 October through 5 November 2008 in which high speed in situ measurements of water vapor and its isotopes were taken at the Mauna Loa observatory and compared to targeted observations from the Aura TES instrument. This inter-comparison approach was developed because the vertical sensitivity of the TES HDO/H_2O ratio peaks at approximately 700 hPa, which is close to the altitude of Mauna Loa (3.1 km, 680 hPa).

Two types of comparisons are made: (1) the observations from directly targeting the TES instrument at the Mauna Loa observatory are directly compared to the in situ data. Vertical information of HDO and H_2O are inferred from the in situ measurements by using the diurnal altitude variability of the planetary boundary layer to map in situ measurements of HDO and H_2O to a profile of HDO and H_2O. This altitude distribution is then compared to the TES HDO/H_2O estimates by passing the constructed profile through the TES "instrument operator", which is a function of the observation averaging kernel and a priori constraint (e.g., Worden et al., 2007). (2) Satellite observed distributions, within 1000 km of Mauna Loa, of the TES HDO/H_2O relative to H_2O are compared against this same distribution of measurements from Mauna Loa. The distribution is obtained from a campaign in which the TES instrument was directed to take several augmenting observations over the entire north Pacific Ocean (Step-and-Stare Mode); these observations are in addition to its nominal observations that are taken over the whole globe every other day (the TES Global Survey mode).

ACPD
10, 25355–25388, 2010

2 Data

2.1 In situ measurements

The NOAA Mauna Loa Observatory site is difficult for in situ sampling of water vapor isotopes because it typically sits above the subtropical PBL where the air can be very dry (e.g., Webster and Heymsfield, 2003). Consequently we used a number of measurement approaches for cross-comparison with each other in addition to comparisons with TES. These included a cavity ringdown spectrometer (CRDS) from Picarro (http://www.picarro.com/) (Gupta et al., 2009) and an off-axis integrated cavity output spectrometer (ICOS) from Los Gatos Research (LGR) (http://www.lgrinc.com/) (Lis et al., 2008). The LGR and Picarro data have been corrected using in situ flask measurements taken at Mauna Loa during the TES overpasses as discussed in Johnson et al. (2010). An average of the corrected high speed data are shown in Fig. 1.

2.2 TES data

As discussed in Beer et al. (2001) and Worden et al. (2004), the Tropospheric Emission Spectrometer is an infrared Fourier transform spectrometer (FTS) that measures the spectral infrared (IR) radiances between 650 cm^{-1} and 3050 cm^{-1} in a limb-viewing and a nadir (downward-looking) mode. The observed IR radiance is imaged onto an array of sixteen detectors that have a combined horizontal footprint of 5.3 km by 8.4 km in the nadir viewing mode. In the nadir view, TES estimates of atmospheric distributions provide vertical information of the more abundant tropospheric species such as H_2O, HDO, O_3, CO, and CH_4 (e.g., Worden et al., 2004). However, sufficient spectral resolution and signal-to-noise ratio are required to distinguish between trace-gas amounts at different altitudes because vertical information about trace gas concentrations is obtained only from spectral variations along the line-of-sight. Consequently, the TES spectral resolution was chosen to match the average pressure-broadened widths of weak infrared molecular transitions in the lower troposphere for nadir measurements (0.06 cm^{-1} apodized) (Beer et al., 2001).

ACPD
10, 25355–25388, 2010

The vertical resolution and error characteristics for the HDO/H_2O estimates from TES are discussed in Worden et al. (2006). Briefly, under clear-sky conditions in the tropics, TES estimates of the HDO/H_2O ratio are sensitive to the distribution of the actual ratio from the surface (~1000 hPa) to about 300 hPa with peak sensitivity at 700 hPa. The sensitivity decreases with latitude through its dependence on temperature and water amount. We estimate a precision of approximately 1% to 2% for the TES estimate of the HDO/H_2O ratio. In addition, Worden et al. (2006) estimated that there was a bias of approximately 5% for column averaged HDO/H_2O estimates between 850 and 500 hPa, where the TES HDO estimates are typically most sensitive by comparing distributions of the TES data to models and aircraft.

3 Direct comparison of TES satellite profile data to in situ data

We compare a TES profile measurement of the HDO/H_2O ratio to a constructed profile of the HDO/H_2O ratio using the Mauna Loa in situ data. Figure 1 shows strong diurnal variability in the HDO/H_2O ratio and in H_2O. During the day, values of the HDO/H_2O ratio are equivalent to PBL values but during the night they are representative of free tropospheric conditions. A profile of HDO and H_2O is constructed from these in situ measurements by mapping these daily variations to a pressure grid by comparing the in situ H_2O to the TES H_2O. Effectively, the vertical movement of the planetary boundary layer is used to construct a vertical profile of HDO and H_2O. The approach for this mapping is discussed in the next section. Comparison of the in situ to the remotely sensed HDO/H_2O profile must also account for the sensitivity of the TES HDO/H_2O measurement to the true distribution of the HDO/H_2O ratio and to the a priori constraint used in the retrieval (e.g., Worden et al., 2006).

Once a profile is constructed, the comparison follows the approach described by Worden et al. (2007b), for the TES ozone profiles except that we must account for the cross correlations in the joint HDO/H_2O profile retrieval used operationally by the TES

ACPD
10, 25355–25388, 2010

algorithm, e.g.:

$$\hat{\boldsymbol{x}}_R = \boldsymbol{x}_a^R + (\mathbf{A}_{DD} - \mathbf{A}_{HD})(\boldsymbol{x}_D - \boldsymbol{x}_a^D) - (\mathbf{A}_{HH} - \mathbf{A}_{DH})(\boldsymbol{x}_H - \boldsymbol{x}_a^H) \quad (1)$$

Where, $\mathbf{A}_{DD}$ and $\mathbf{A}_{HH}$ are the averaging kernel matrices for HDO and H_2O separately (available in the individual product files for those species). The $\mathbf{A}_{HD}$ and $\mathbf{A}_{DH}$ are the cross averaging kernels between HDO and H_2O and the reverse; these matrices are available in the Ancillary product files. Note that the averaging kernels are not symmetric so one cannot use one cross term for the other. The $\boldsymbol{x}_\mathbf{D}$, $\boldsymbol{x}_\mathbf{H}$, are the "true" distribution of HDO and H_2O, respectively and are represented as the log of the concentration of each species (given in volume mixing ratio), $\boldsymbol{x}$=log($\boldsymbol{q}$), where $\boldsymbol{q}$ is the volume mixing ratio of H_2O or HDO. The $\boldsymbol{x}_a$ is the a priori constraint vector for each species (available in the product files). We have not included error terms related to interfering species or noise in Eq. (1); these error terms are discussed in Worden et al. (2006) and will be quantified in Sect. 3.3. For this analysis, the "true" HDO and H_2O values will be constructed from the in situ data shown in Fig. 1.

After passing the "true" HDO and H_2O and constraint vector profiles through the averaging kernels, the "true" HDO/H_2O ratio (or actually log[HDO/H_2O]), $\hat{\boldsymbol{x}}_R$, will have been adjusted to account for the sensitivity of the TES estimate to HDO and H_2O and also to the bias introduced into the retrieval via the constraint vector that is used to regularize the retrieval; the error from this bias and vertical resolution is also called "smoothing error" (Rodgers, 2000) As shown in Worden et al. (2007b) for the TES ozone retrievals, and in Worden et al. (2006) for the HDO/H_2O retrievals, the difference between this modified "true" ratio and the measurement from TES is due to any un-quantified biases in the TES data as well as the measurement uncertainty due to noise and other geophysical parameters that affect the TES HDO/H_2O retrieval such as temperature, emissivity, and clouds.

ACPD
10, 25355–25388, 2010

3.1 Comparison of in situ data to TES HDO/H_2O profiles

We next describe the approach for comparing the in situ data to the HDO/H_2O profiles. We only used those TES observations that were taken directly over the Mauna Loa observatory because we found that the variability in the H_2O and HDO/H_2O estimates for the 32 observations along the TES transect was larger than the expected error in the bias. To corroborate the reasons for this variability, Fig. 2 shows the cloud field over Mauna Loa, as measured by the Aqua Moderate Resolution Imaging Spectroradiometer (MODIS) instrument (e.g., Barnes et al., 1998), on 20 October 2008, approximately 02:00 p.m. LT. While most of the island is covered in clouds, the air directly above the Mauna Loa volcano and NOAA observatory are apparently cloud free; this information from the MODIS visible light measurement is consistent with the estimated cloud optical depth of 0.08 from the TES estimate directly over Mauna Loa. In addition, Fig. 3 (left panel) shows H_2O profiles from a nearby sonde launched from Hilo and also Lihue, approximately 500 km NW of Mauna Loa. The sonde data is downloaded from a U. of Wyoming resource (http://weather.uwyo.edu/upperair/sounding.html). The sondes are typically launched over the ocean and show humidity profiles that are much drier than that measured directly over Mauna Loa by TES. However, the bottom level of the TES H_2O profile agrees well with the in situ measurement from the average of the Picarro and LGR data (square symbol). As can be seen in the left panel of Fig. 4, the TES H_2O estimate is most sensitive to the air directly above Mauna Loa and the error on this estimate is approximately 7% indicating that good agreement should be expected. Because of the variability in clouds and water vapor concentrations around Mauna Loa we conclude that we can only compare the in situ data from Mauna Loa to TES observations directly over Mauna Loa.

Only three daytime observations (out of five total direct TES observations) could be used for inter-comparison with the in situ data. These observations were taken on 20 October and 22 and 5 November 2008. Two night-time measurements could not be directly used because the sensitivity was too low due to cold temperatures and clouds.

ACPD
10, 25355–25388, 2010

We next describe the approach for comparing the in situ data to the 20 October 2008 TES observation.

3.2 Construction of HDO/H_2O profile from in situ data

As noted earlier, the altitude variability of the boundary layer height is used to construct the altitude profile of the HDO/H_2O ratios for use in Eq. (1). This HDO/H_2O profile is constructed using the high speed H_2O in situ measurements interpolated to the TES pressure grid using the TES H_2O profile:

$$P_{\mathrm{TES}}(\mathrm{H_2O_{in\,situ}}) = M(\mathrm{H_2O_{in\,situ}}, \mathrm{H_2O_{TES}}, P_{\mathrm{TES}}) \quad (2)$$

Where $P_{\mathrm{TES}}(\mathrm{H_2O_{in\,situ}})$ is the equivalent pressure on the TES pressure grid for the measured in situ H_2O. The $\mathrm{H_2O_{in\,situ}}$ and $\mathrm{H_2O_{TES}}$ are the in situ and TES measured H_2O values, and P_{TES} is the TES forward model pressure grid. The M is a mapping relationship that is constructed using the following steps:

1) Obtain in situ HDO and H_2O data corresponding to satellite overpass. An example of these data from the Picarro/LGR average for 20 October is shown in Fig. 4.

2) Identify where the TES H_2O data at each pressure level (diamonds in left panel of Fig. 3 and dotted lines in Fig. 5) matches to the in situ data. Note that in this instance only the first 5 pressure levels are used because H_2O amounts lower than 0.001 VMR are not measured by the Picarro and LGR instruments.

3) Average all delta-D values from the corrected Picarro/LGR data where the TES and in situ H_2O values agree to within 5%; these delta-D values for the first five pressure levels correspond approximately to the dotted lines in the bottom of Fig. 5. After this step we have matching delta-D/pressure pairs that can be used to construct a delta-D profile. The 5% threshold was chosen ad hoc to balance the number of corresponding in situ H_2O measurements that could be compared to the TES H_2O versus increasing the representation error by increasing the threshold. This mapping also makes the assumption that the observed

ACPD
10, 25355–25388, 2010

air parcels measured over the day by the in situ device is representative of the observed air parcel measured at a single time by TES. We estimate the error from these assumptions as the variability of the in situ HDO/H_2O measurement for the range of in situ H_2O measurements that are within 5% of the TES H_2O values at each pressure level; typically these errors range from 3 to 15 per mil and are included in the total error budget as a random error (Sect. 3.3). As seen in Fig. 4, the first 5 pressure levels span almost all the pressure levels where the H_2O and HDO estimates are most sensitive, as indicated by their averaging kernel matrices.

4) Construct the delta-D profile using the matching H_2O values from Step 3; the lower troposphere values correspond to the TES pressure levels indicated by diamonds in Fig. 3. For the range of pressures (or altitudes) for which we do not have corresponding in situ and TES measurements of H_2O we interpolate between the in situ measurements (noted as diamonds in Fig. 4) to the a priori constraint vector at 200 hPa.

5) Calculate the "true" HDO profile using the TES H_2O profile from the left panel in Fig. 2 and the "true" delta-D profile shown as the green line in the right panel of Fig. 2. Note that we are effectively interpolating HDO and H_2O in the middle/upper troposphere where there are no corresponding in situ measurements; this approximation incurs an error that is equivalent to the "smoothing" error related to use of the a priori constraint and vertical resolution of the estimate for this part of the atmosphere. We conservatively add in the smoothing error of the whole profile, not just the part due to this part of the atmosphere, to the total error budget in order to account for this interpolation.

6) The last step involves transforming the HDO and H_2O profiles with the combined HDO/H_2O averaging kernel matrix using Eq. (1). The modified estimate for HDO and H_2O can now be compared to the TES estimate as it accounts for the TES sensitivity and a priori bias; this is shown as the red line in the right panel of Fig. 3.

ACPD
10, 25355–25388, 2010

3.3 Error characterization

As shown in Worden et al. (2006), the total error due to noise and geophysical parameters affecting the observed radiances (e.g. temperature, emissivity, and clouds) are described by the following equation:

$$\mathbf{S}_{\text{obs}} = \mathbf{S}_{\text{meas}} + \sum_i \mathbf{S}_i^{\text{int}} \tag{3}$$

where S_{meas} is the measurement error due to noise and the summation, $\sum_i S_i^{\text{int}}$, is the sum of all interfering parameters such as temperature and clouds affecting the retrieval. These covariance matrices are also present in the product files. As shown in Worden et al. (2006) The sum of these errors for the HDO/H_2O ratio is:

$$\mathbf{S}_{\text{R}} = \mathbf{S}_{\text{DD}} + \mathbf{S}_{\text{HH}} - 2\mathbf{S}_{\text{DH}} \tag{4}$$

where S_{DD} is the covariance for HDO (measurement, total, or observation), S_{HH} is the covariance for water, and is the cross term; these covariances are given for measurement, total, and observation errors in the individual product files. As noted in Worden et al. (2006), the cross term is subtracted off from the sum of the HDO and H_2O covariances because the HDO and H_2O profiles are jointly estimated from the same measurement. Unlike the averaging kernel matrix, the covariance matrices are all symmetric.

In addition to the errors in the estimate from the TES measurement there are also errors in how the "true" HDO concentrations are constructed as discussed in Step 3 in Sect. 3.2. These errors are calculated using the approach in Step 3 and are assumed to be randomly distributed. On the assumption that this error affects only the calculation of the "true" HDO profile its impact on the total error budget (Worden et al., 2004, 2006) is:

$$\mathbf{S}_{\text{in situ}}^{\text{profile}} = \mathbf{A}_{\text{DD}} \mathbf{S}_{\text{in situ}} \mathbf{A}_{\text{DD}}^{\text{T}} \tag{5}$$

ACPD
10, 25355–25388, 2010

where the diagonals of $\mathbf{S}_{\text{in situ}}$ is populated by the errors calculated in Step 3 and $\mathbf{S}^{\text{profile}}_{\text{in situ}}$ is added into the total error budget as shown in Eq. (3). Note that this error, after smoothing by the HDO component of the averaging kernel as shown in Eq. (5) typically adds approximately 10–15 per mil to the total error budget.

The comparison of the TES HDO/H_2O estimate to the constructed profile, modified by the constraint vector and averaging kernel as shown in Eq. (1), should ideally agree to within these random errors and the bias estimate.

3.4 Bias correction

Worden et al. (2006) found that the TES HDO/H_2O ratios were likely biased by approximately 5–6% by comparing distributions of the HDO/H_2O ratio with model and aircraft data. Our primary objective of the Mauna Loa validation experiment is to characterize the bias in the HDO/H_2O ratio. We assume that the bias in the TES HDO data is due to uncertainties in the spectroscopic line strengths (e.g., Toth, 1999; Webster and Heymsfeld, 2003). The correction for this bias must therefore account for the sensitivity of the retrieval since a bias in the line strengths would be similar to an offset in the retrieved HDO concentration. For example, if the TES HDO estimate showed zero sensitivity then the estimate would return to the a priori constraint regardless of the spectroscopic uncertainties. For this reason we use the following form for the bias correction as discussed in Worden et al. (2007a):

$$\ln(\boldsymbol{q}^{\text{HDO}}_{\text{corrected}}) = \ln(\boldsymbol{q}^{\text{HDO}}_{\text{original}}) - \mathbf{A}_{\text{DD}}(\boldsymbol{\delta}_{\text{bias}}) \quad (6)$$

where is the volume mixing ratio of the HDO profile as provided in the product files, $\mathbf{A}_{\text{DD}}$ is the averaging kernel matrix (also provided in the product files), and is a column vector of the same length as that contains the bias correction. Note that this correction is only applied to HDO and not to H_2O. This bias term is calculated by comparison of the TES HDO/H_2O estimates to constructed profiles of the HDO/H_2O ratio using the in situ data from the Picarro and LGR instruments. It is also quite likely that there is

ACPD
10, 25355–25388, 2010

a bias error in the H_2O spectral absorption coefficients; however it would be difficult to separately resolve these two errors and therefore for simplicity we aggregate this error into the HDO line strengths.

3.5 Summary of direct comparison between TES and in situ data

Bias corrections are found by simply correcting the TES HDO profiles with a bias value until the corrected TES estimate and the "true" HDO/H_2O profile, modified by the averaging kernel and a priori constraint, agree "by eye" within the estimated uncertainties; a more formal line-fit is unnecessary as it would not improve on our description of the errors. The average of the bias corrections for the three TES profiles used in the direct comparisons is 0.056; with the three bias estimates being 6%, 5.7%, and 5%; the differences between these three bias corrections is well within the expected random error related to the TES data and the error in the constructed true profile of approximately 2%. We next discuss an indirect comparison between the TES data and the in situ data that corroborates these findings.

4 Indirect comparison of TES data to in situ data

Another method for comparing the TES data to the in situ data is to compare there respective delta-D versus H_2O distributions for a large number of observations. This makes use of the expectation that the free tropospheric water vapor observed by TES around Hawaii should, on average, have a similar moist process history as the water vapor observed in situ at Mauna Loa. Figure 6 shows distributions of delta-D versus H_2O using the in situ measurements from Picarro and LGR and all TES data taken during October 2008 that was within 1000 km of Hawaii. Only data where the degrees-of-freedom for signal for HDO is larger than 0.5 is used. Then, the TES HDO profiles are corrected for biases of 0.02, 0.05, 0.056, 0.06, and 0.07. After this bias correction the HDO/H_2O profiles are constructed and a column average is calculated for each

ACPD
10, 25355–25388, 2010

profile using the pressure range between 825 hPa and 464 hPa. These column averages, using the different bias corrections, are then compared to the delta-D versus H_2O distributions from the Picarro/LGR in situ. What we can conclude from this comparison is that the TES HDO data should be corrected by at least 0.056% in order for ~99% of the TES HDO/H_2O distribution to be within the in situ distribution. Unfortunately, we cannot exactly compare these distributions since the TES data, as seen in the averaging kernels (Fig. 4) are representative of both PBL and free tropospheric air whereas the in situ data will have a different distribution that depends on the time-of-day and variability of the PBL height. Consequently, it is possible based on the comparison shown in Fig. 6, that the bias correction could be larger than 0.056. However, a larger correction would be inconsistent with the vertical profile comparisons shown in the last section and the Appendix.

5 Comparison between Version 4 and Version 3

In this section we compare delta-D values between Version 4 and Version 3 of the TES isotope data. A significant difference between these versions is that the temperature retrieval strategy was changed in order to obtain improved atmospheric temperatures. Because the spectral absorption lines for both HDO and H_2O are temperature sensitive, this change will impact the HDO and H_2O estimates. Although these changes are likely due to temperature we can partially correct for them using the same approach as described in Eq. (1). After correcting for a 1.5 percent bias between the versions, the mean difference between versions is reduced from 8.8 ppm to −2.2 ppm, as shown in Fig. 7. Note that there is a residual latitudinal difference at higher latitudes because this correction cannot completely account for the differences in the two versions due to the differences in the temperature retrieval.

ACPD
10, 25355–25388, 2010

6 Summary

HDO/H_2O estimates from TES radiance measurements taken directly over the Mauna Loa observatory were compared to in situ data at the Mauna Loa observatory. By using the vertical movement of the PBL during the day we could interpolate in situ measurements of H_2O and HDO to the TES pressure grid in the lower troposphere. This constructed altitude profile could then be compared to the TES estimates of HDO after accounting for the TES sensitivity and a priori constraint. The estimated bias error for the three constructed profiles available for this comparison were 5.5%, 6%, and 5.7% with an average value between these three comparisons of 5.56%. We estimated that the uncertainties at any given level for the constructed in situ and TES profiles ranged from 0.5% to 2%. Consequently, it is very likely that the error in this bias estimate is less than 2% and given the spread in the bias estimates, the error in the bias estimate is likely less than 1%.

We also indirectly compared the TES HDO/H_2O estimates by calculating averages of the HDO/H_2O ratio between 825 and 464 hPa from TES measurements within 1000 km of Mauna Loa during this validation campaign and comparing them to the distribution of H_2O versus the HDO/H_2O ratio. While the two distributions could not exactly be compared we found that the TES HDO concentrations should be reduced by at least 5.56% in order for the two distributions to be consistent. However, this comparison approach is not completely robust because greater reductions in the TES HDO could also be made and the two distributions would still be consistent.

Finally, we compared Version 3 to Version 4 data and found that the version 3 data should be bias corrected by 4%. As with Version 4 data, this bias correction should not be directly applied to the HDO/H_2O ratio but instead be applied to the HDO profile and account for the TES HDO sensitivity and a priori constraint.

Acknowledgement. The work described here is performed at the Jet Propulsion Laboratory, California Institute of Technology under contracts from the National Aeronautics and Space Administration. The NASA ROSES Aura Science Team NNH07ZDA001N-AST 07-AST07-0069

contributed to the support of the analysis. The Mauna Loa field program was supported by NSF Grants ATM-084018 to Joe Galewsky and ATM-0840129 to David Noone. The views, opinions, and findings contained in this report are those of the author(s) and should not be construed as an official National Oceanic and Atmospheric Administration or US Government position, policy, or decision.

Appendix A

In this section we show comparisons between the 22 October and 5 November TES HDO/H_2O measurements and the corresponding in situ data. As seen in Figs. A1 and A5 both measurements show significant cloud coverage and these visible light measurements are corroborated by the estimated cloud effective optical depth of 0.92 and 1.3, respectively and the estimated cloud top heights from TES as seen in Figs. A3 and A7. However the cloud optical depths are small enough such that the TES estimates are sensitive to the HDO/H_2O ratio below the cloud as seen in the averaging kernels for these observations (Figs. A4 and A8). Using the method described in Sect. 3 for constructing a "true" in situ HDO/H_2O profile, we find good agreement between the TES data and the in situ data if a bias correction of 0.056 is applied to the TES data using Eq. (6).

References

Barnes, W. L., Pagano, T. S., and Salomonson, V. V. Prelaunch characteristics of the Moderate Resolution Imaging Spectroradiometer (MODIS) on EOS-AM1, IEEE T. Geosci. Remote, 36, 1088–1100, 1998.

Beer, R., Glavich, T. A., and Rider, D. M.: Tropospheric emission spectrometer for the Earth Observing System's Aura Satellite, Appl. Optics, 40, 2356–2367, 2001.

Brown, D., Worden, J., and Noone, D.: Comparison of atmospheric hydrology over convective continental regions using water vapor isotope measurements from space, J. Geophys. Res.-Atmos., 113, D15124, doi:10.1029/2007JD009676, 2008.

ACPD

10, 25355–25388, 2010

Craig, H.: Isotopic variations in meteoric waters, Science, 133, 1702, 1961.
Dansgaard, W.: Stable isotopes in precipitation, Tellus, 16, 436–468, 1964.
Frankenberg, C., Yoshimura K., Warneke T., et al.: Dynamic Processes Governing Lower-Tropospheric HDO/H2O Ratios as Observed from Space and Ground, Science, 325, 1374–1377, 2009.
Galewsky, J., Strong, M., and Sharp, Z.: Measurements of water vapor D/H ratios from Mauna Kea, Hawaii, and implications for subtropical humidity dynamics, Geophys. Res. Lett., 34, L22808, doi:10.1029/2007GL031330, 2007.
Gupta, P., Noone, D., Galewsky, J., Sweeny, C., and Vaughn, B. H.: Demonstration of high precision continuous measurements of water vapor isotopologues in laboratory and remote field deployments using WS-CRDS technology, Rapid. Commun. Mass. Sp., 23(16), 2534–2542, doi:10.1002/rcm.4100, 2009.
Herbin, H., Hurtmans, D., Turquety, S., Wespes, C., Barret, B., Hadji-Lazaro, J., Clerbaux, C., and Coheur, P.-F.: Global distributions of water vapour isotopologues retrieved from IMG/ADEOS data, Atmos. Chem. Phys., 7, 3957–3968, doi:10.5194/acp-7-3957-2007, 2007.
Herbin, H., Hurtmans, D., Clerbaux, C., Clarisse, L., and Coheur, P.-F.: $H_2{}^{16}O$ and HDO measurements with IASI/MetOp, Atmos. Chem. Phys., 9, 9433–9447, doi:10.5194/acp-9-9433-2009, 2009.
Kuang, Z. M., Toon, G. C., Wennberg, P. O., and Yung, Y. L.: Measured HDO/H2O ratios across the tropical tropopause, Geophys. Res. Lett., 30, 1372, doi:10.1029/2003GL017023, 2003.
Johnson, L. R., Sharp, Z., Galewsky, J., Strong, M., Gupta, P., Baer, D., and Noone, D.: Hydrogen isotope measurements of water vapor and a correction for laser instrument measurement bias at low water vapor concentrations: applications to measurements from Mauna Loa Observatory, Hawaii, in preperation, 2010.
Lee, J. E., Pierrehumbert, R., Swann, A., and Lintner, B. R.: Sensitivity of stable water isotopic values to convective parameterization schemes, Geophys. Res. Lett., 36,, L23801, doi:10.1029/2009GL040880, 2009.
Lis, G., Wassenaar, L. I., and Hendry, M. J.: High-precision laser spectroscopy D/H and O-18/O-16 measurements of microliter natural water samples, Anal. Chem., 80, 287–293, 2008.
Moyer, E. J., Irion, F. W., Yung, Y. L., and Gunson, M. R.: ATMOS stratospheric deuterated water and implications for troposphere-stratosphere transport, Geophys. Res. Lett., 23, 2385–

ACPD
10, 25355–25388, 2010

2388, 1996.
Nassar, R., Bernath, P. F., Boone, C. D., Gettelman, A., McLeod, S. D., and Rinsland, C. P.: Variability in HDO/H2O abundance ratios in the tropical tropopause layer, J. Geophys. Res., 112, D21305, doi:10.1029/2007JD008417, 2007.
Payne, V. H., Noone, D., Dudhia, A., Piccolo, C., and Grainger, R. G.: Global satellite measurements of HDO and implications for understanding the transport of water vapour into the stratosphere, Q. J. Roy. Meteor. Soc., 133, 1459–1471, 2007.
Risi, C., Bony, S., and Vimeux, F.: Influence of convective processes on the isotopic composition (delta O-18 and delta D) of precipitation and water vapor in the tropics: 2. Physical interpretation of the amount effect, J. Geophys. Res.-Atmos., 113, D19306, doi:10.1029/2008JD009943, 2008.
Schneider, M., Hase, F., and Blumenstock, T.: Ground-based remote sensing of HDO/H_2O ratio profiles: introduction and validation of an innovative retrieval approach, Atmos. Chem. Phys., 6, 4705–4722, doi:10.5194/acp-6-4705-2006, 2006.
Steinwagner, J., Fueglistaler, S., Stiller, G., et al.: Tropical dehydration processes constrained by the seasonality of stratospheric deuterated water, Nature Geosci., 3, 262–266, 2010.
Toth, R. A.: HDO and D_2O low pressure, long path spectra in the 600–3100 cm^{-1} region I. HDO line positions and strengths, J. Mol. Spectrosc., 195, 73–97, 1999.
Webster, C. R. and Heymsfield, A. J.: Water isotope ratios D/H, O-18/O-16, O-17/O-16 in and out of clouds map dehydration pathways, Science, 302, 1742–1745, 2003.
Worden, J., Bowman, K., Noone, D., Beer, R., Clough, S., Eldering, A., Fisher, B., Goldman, A., Gunson, M., Herman, R., Kulawik, S., Lampel, M., Luo, M., Osterman, G., Rinsland, C., Rodgers, C., Sander, S., Shephard, M., and Worden, H.: Tropospheric emission spectrometer observations of the tropospheric HDO/H_2O ratio: estimation approach and characterization, J. Geophys. Res., 111, D16309, doi:10.1029/2005JD006606, 2006.
Worden, J., Noone, D., Bowman, K., and TES science team and data contributors: Importance of rain evaporation and continental convection in the tropical water cycle, Nature, 445, 528–532, doi:10.1038/nature05508, 2007a.
Worden, H. M., Logan, J. A., Worden, J. R., Beer, R., Bowman, K., Clough, S. A., Eldering, A., Fisher, B. M., Gunson, M. R., Herman, R. L., Kulawik, S. S., Lampel, M. C., Luo, M., Megretskaia, I. A., Osterman, G. B., and Shephard, M. W.: Comparisons of tropospheric emission spectrometer (TES) ozone profiles to ozonesondes: methods and initial results, J. Geophys. Res., 112, D03309, doi:10.1029/2006JD007258, 2007b.

ACPD
10, 25355–25388, 2010

Zakharov, V. I., Imasu, R., Gribanov, K. G., Hoffmann, G., and Jouzel, J.: Latitudinal distribution of the deuterium to hydrogen ratio in the atmospheric water vapor retrieved from IMG/ADEOS data, Geophys. Res. Lett., 31, L12104, doi:10.1029/2004GL019433, 2004.

ACPD
10, 25355–25388, 2010

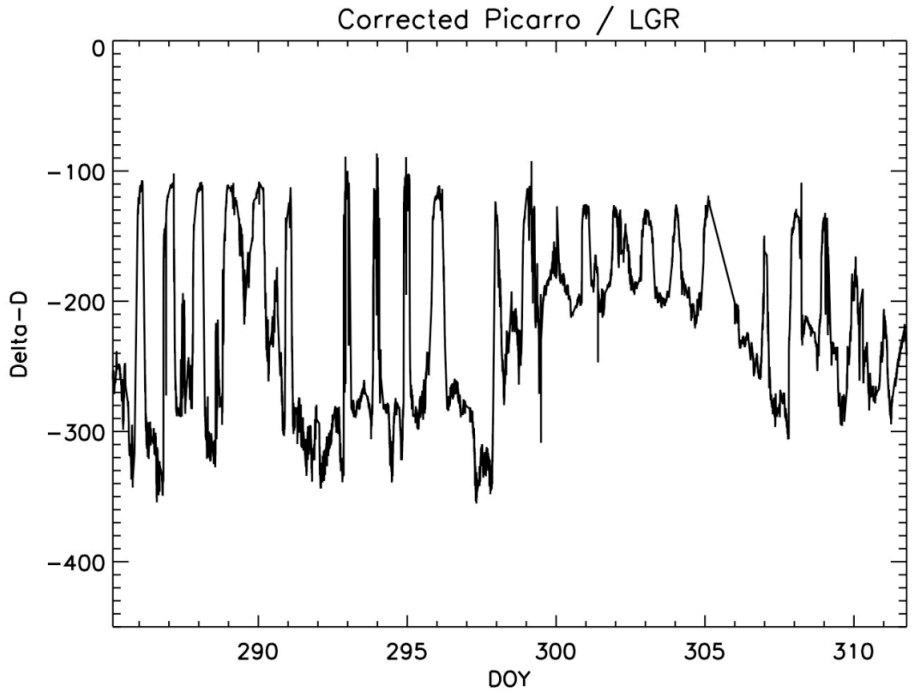

Fig. 1. Corrected time-series from an average of the Picarro/LGR data sets as described in Johnson et al. (2010).

ACPD
10, 25355–25388, 2010

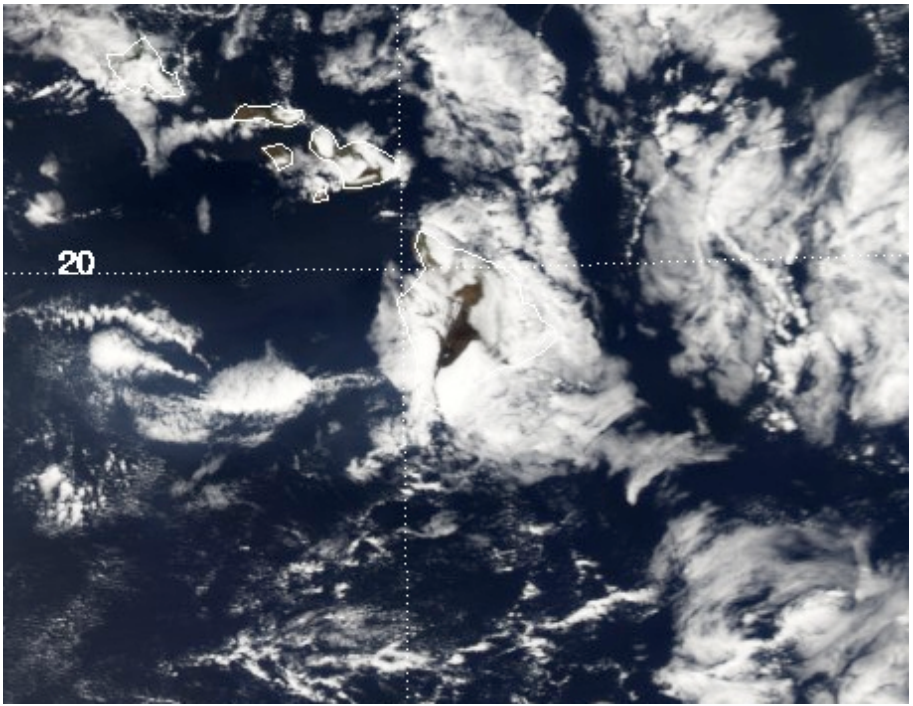

Fig. 2. MODIS clouds for 19 October 2008 23:45 UTC centered over the Big Island of Hawaii.

ACPD
10, 25355–25388, 2010

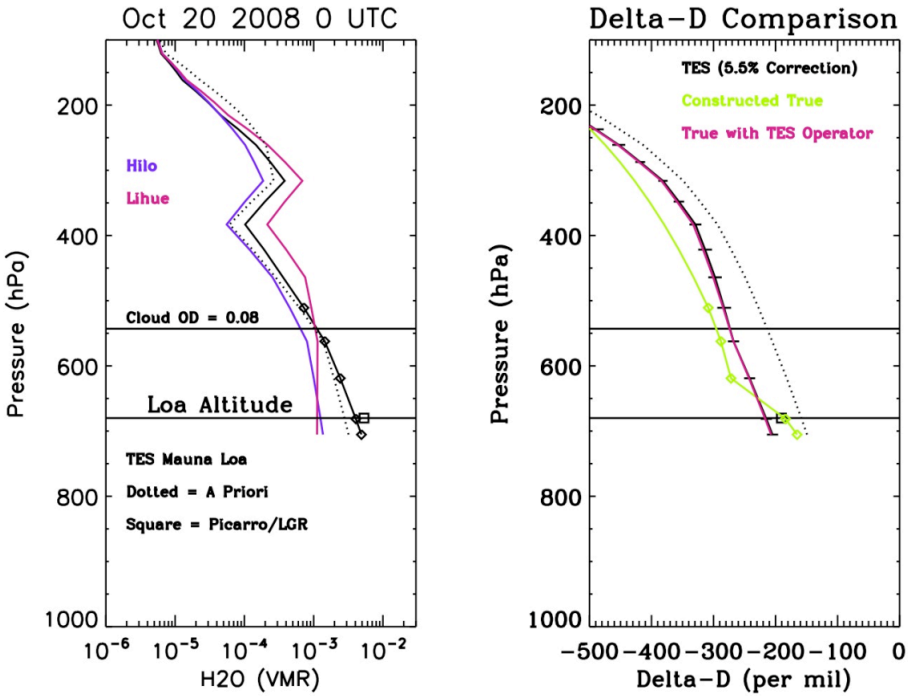

Fig. 3. Left panel: TES and sonde H_2O. The colored solid lines show H_2O measurements from sondes launched in Hilo and Lihue and modified by the TES H_2O averaging kernel and a priori constraint (dotted line). Right panel: The TES Delta-D profile (corrected for bias), the a priori constraint (dotted line), the constructed "true" Delta-D profile (solid green line), and the "true" profile modified by the TES averaging kernel and a priori constraint (solid red line). The error bars are due to measurement and interfering geophysical parameters as well as errors in the constructed "true" profile. The cloud top height is the solid line. Diamonds in both plots refer to the pressure levels used to construct the "true" Delta-D profile. The squares in both plots is the corresponding in situ measurement at the time of the TES overpass.

ACPD
10, 25355–25388, 2010

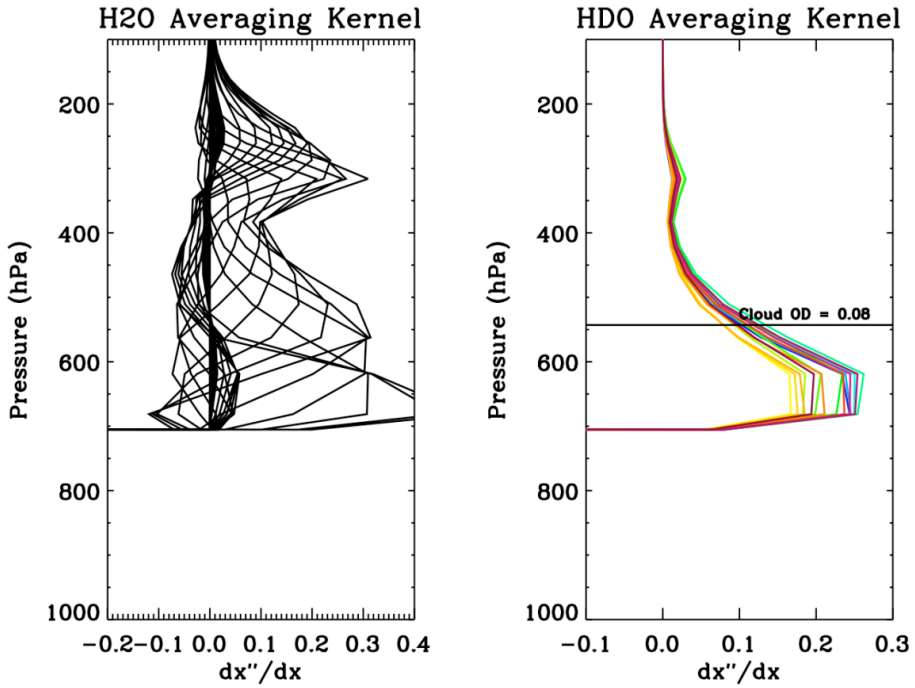

Fig. 4. The averaging kernels (rows of the averaging kernel matrix) for the H_2O and HDO components of the retrieval. The cloud top height is shown as a solid line (with cloud optical depth of 1.3) in the right panel. The colors in the averaging kernel plot indicate pressure level for each averaging kernel row with black and blue being the highest two pressures and red being the lowest pressure.

ACPD
10, 25355–25388, 2010

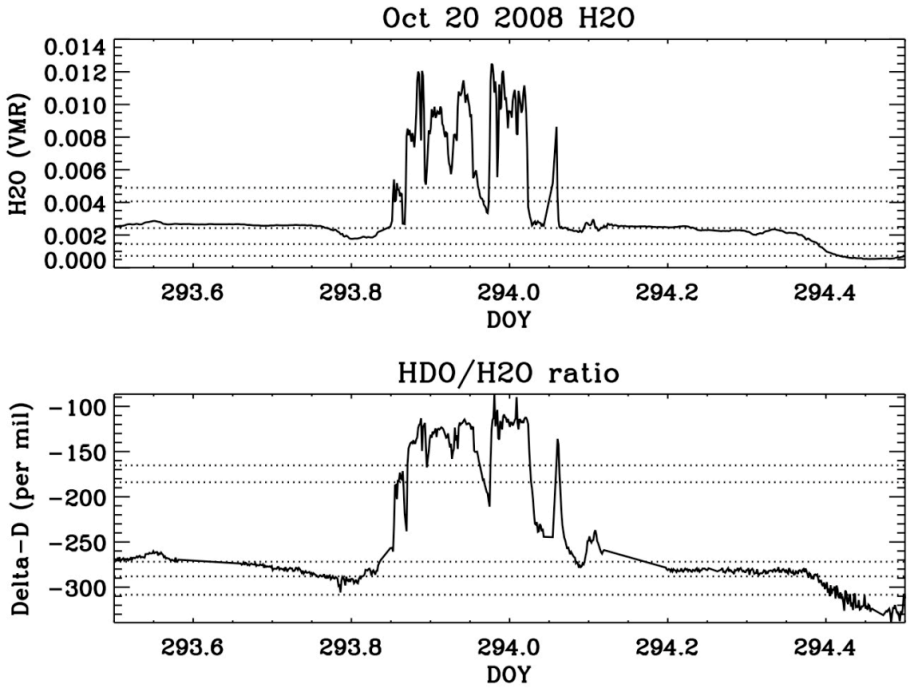

Fig. 5. H_2O (top) and Delta-D (bottom) values derived from averaging the LGR and Picarro measurements. The dotted lines correspond to water values at the first five pressure levels of the TES H_2O profile shown in Fig. 3.

ACPD
10, 25355–25388, 2010

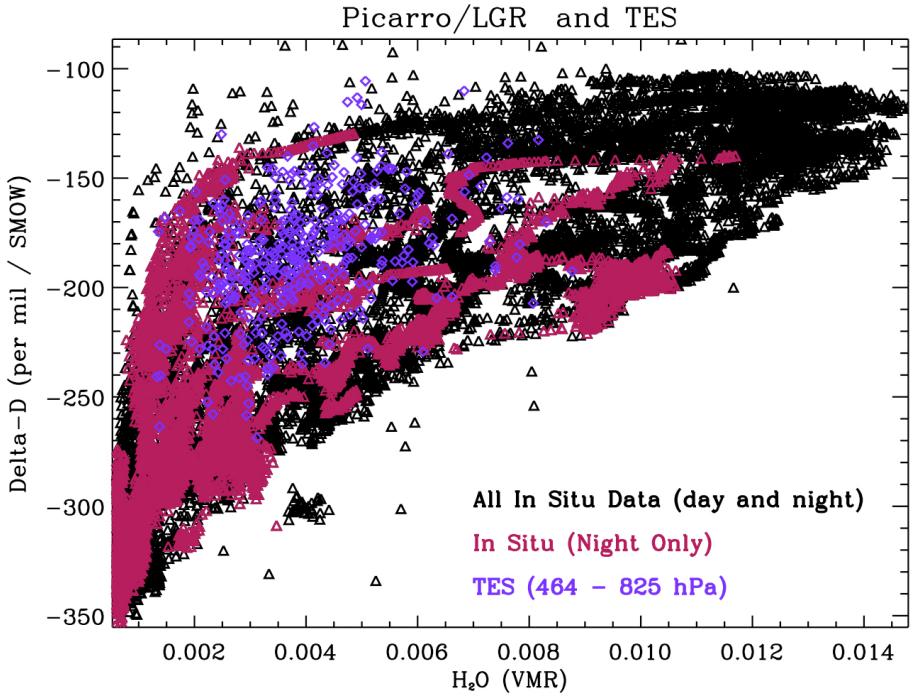

Fig. 6. (Black Diamonds) Distribution of Delta-D versus H_2O from the average of the Picarro and LGR data from 11 October through 5 November 2008. (Red) Night-time values for these same data. (Blue) TES column averages for all data within 1000 km of Hawaii; the TES data have been corrected using a bias correction factor of 0.056, modified by the averaging kernel.

ACPD
10, 25355–25388, 2010

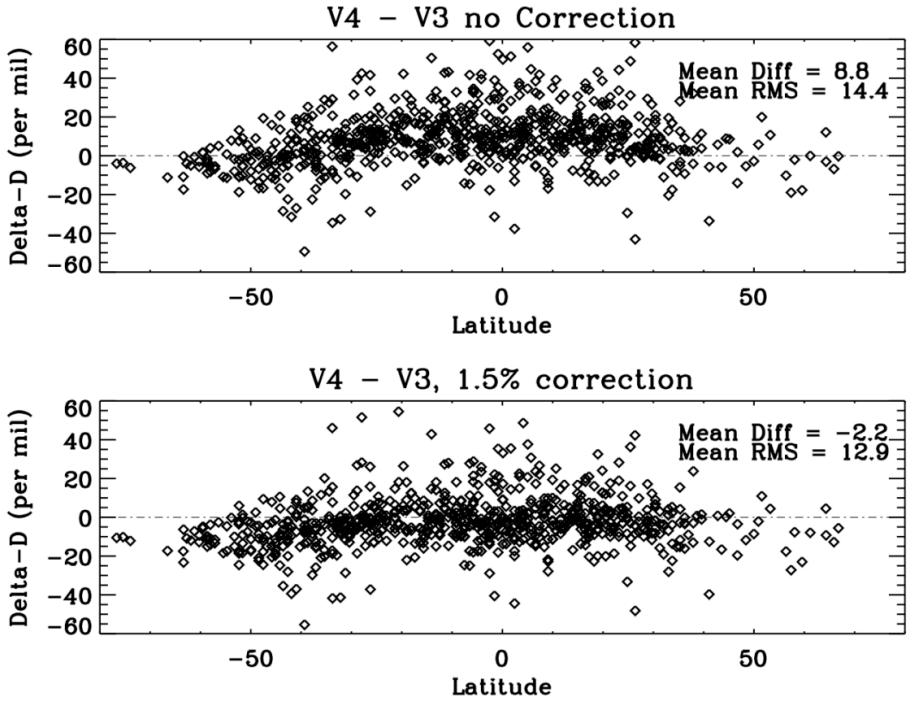

Fig. 7. Comparison between V4 and V3 of the TES HDO/H_2O ratios, averaged between 825 and 500 hPa. The bottom panel includes a 1.5% correction to V4, modified by the HDO averaging kernel.

ACPD
10, 25355–25388, 2010

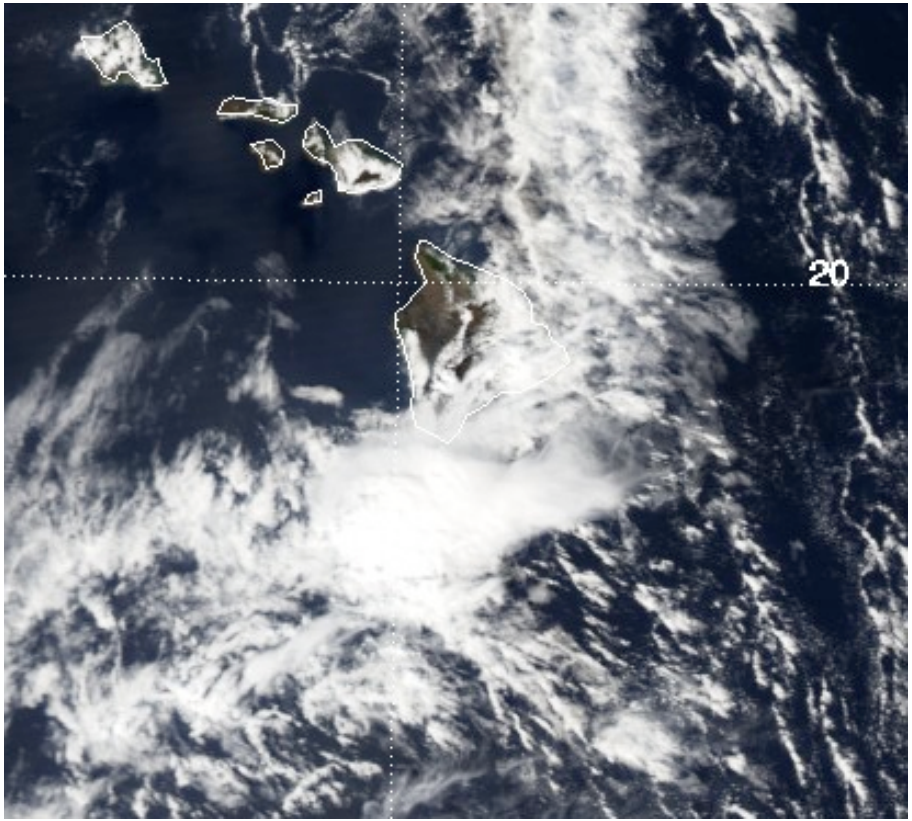

Fig. A1. Aqua MODIS image of the big island of Hawaii for 22 October approximately 00:00 UTC.

ACPD
10, 25355–25388, 2010

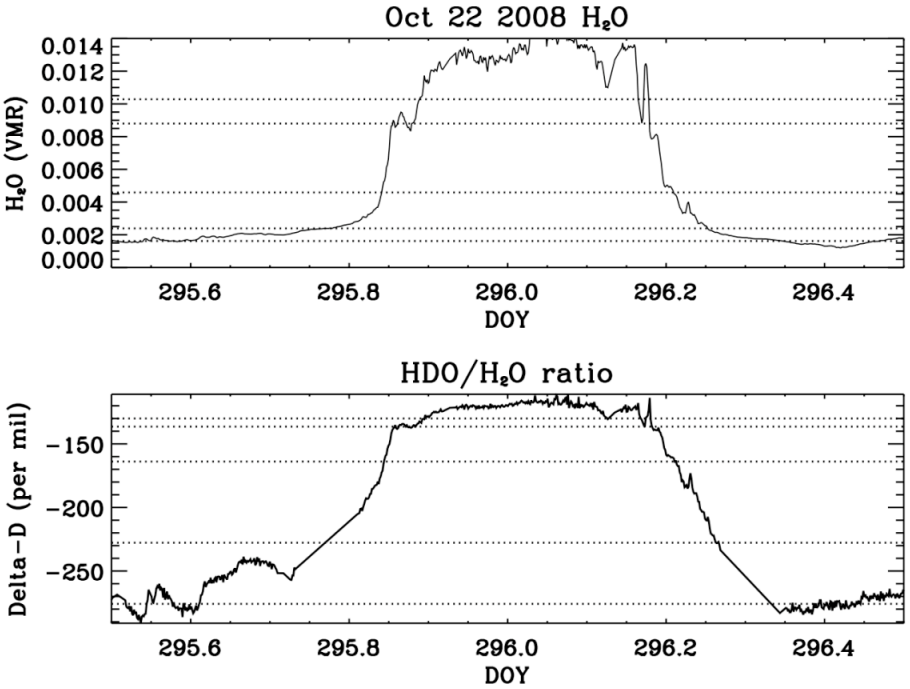

Fig. A2. Solid lines are the averaged values of the Picarro and LGR in situ measurements for H_2O (top) and Delta-D (bottom). The dashed lines indicate the water and Delta-D values used to construct the true HDO/H_2O profile.

ACPD
10, 25355–25388, 2010

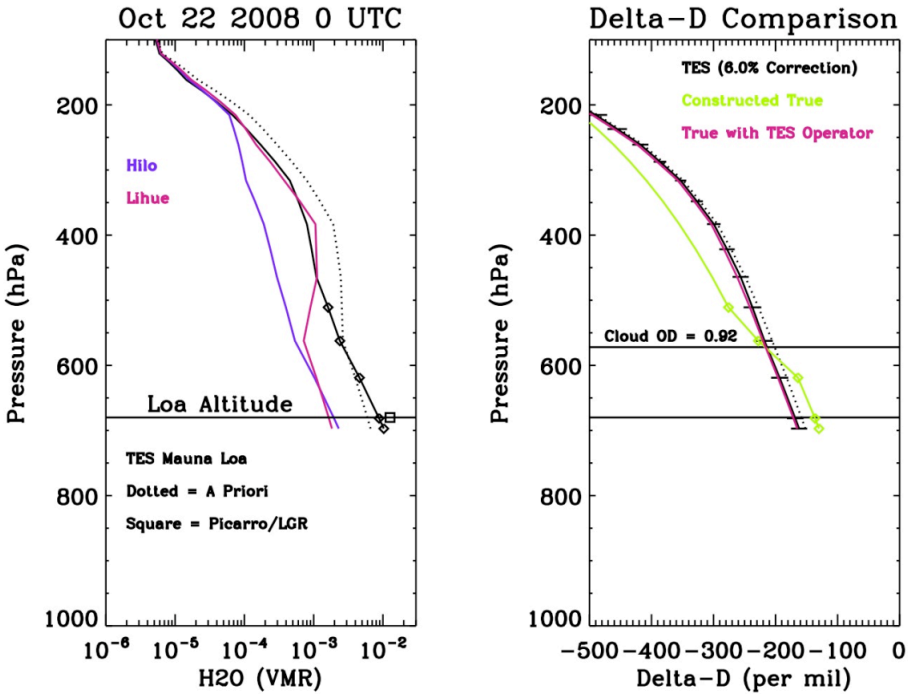

Fig. A3. Left panel: TES and sonde H_2O. The colored solid lines show H_2O measurements from sondes launched in Hilo and Lihue and modified by the TES H_2O averaging kernel and a priori constraint (dotted line). Right panel: the TES Delta-D profile (corrected for bias), the a priori constraint (dotted line), the constructed "true" Delta-D profile (solid green line), and the "true" profile modified by the TES averaging kernel and a priori constraint (solid red line). The error bars are due to measurement and interfering geophysical parameters as well as errors in the constructed "true" profile. The cloud top height is the solid line. Diamonds in both plots refer to the pressure levels used to construct the "true" Delta-D profile. The squares in both plots is the corresponding in situ measurement at the time of the TES overpass.

ACPD
10, 25355–25388, 2010

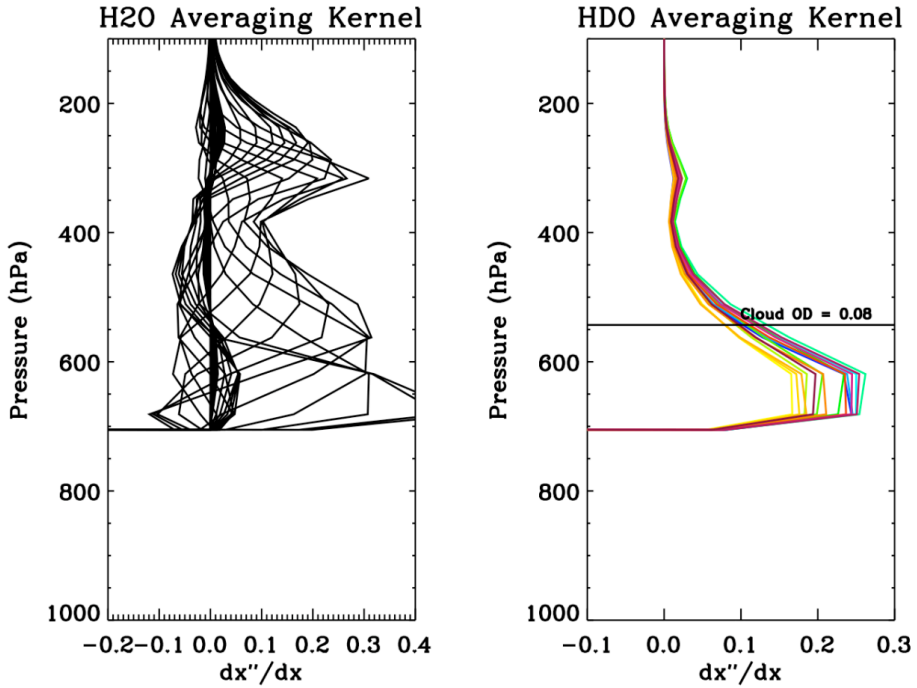

Fig. A4. Left panel: averaging kernels for TES H_2O profile. Right panel: averaging kernels for TES HDO profile. The cloud top height is shown as a solid in the right panel.

ACPD
10, 25355–25388, 2010

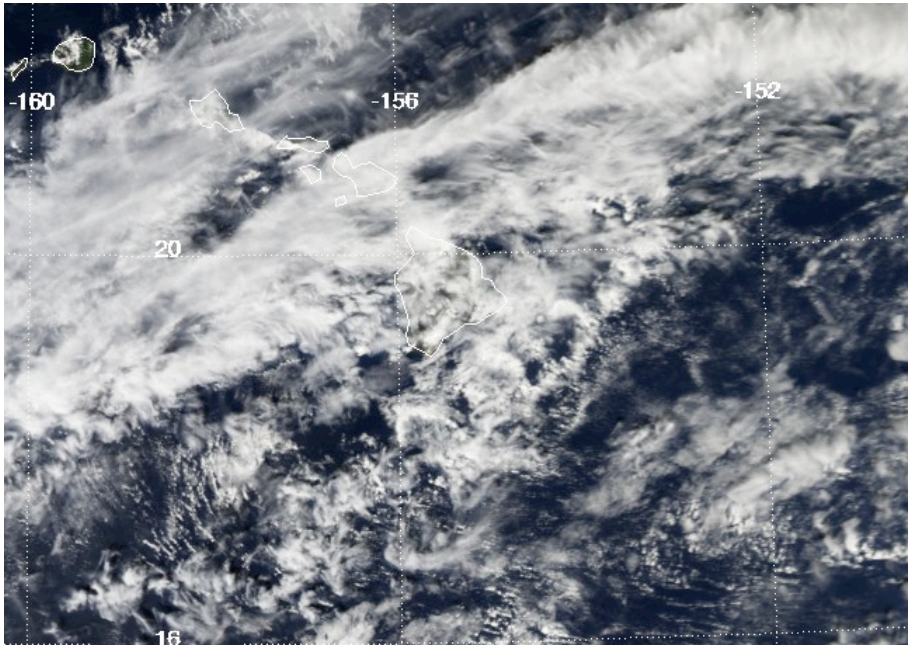

Fig. A5. Aqua MODIS image of the Hawaii islands for 5 November 2008 ~00:00 UTC. The big island is just south of 20° N.

ACPD
10, 25355–25388, 2010

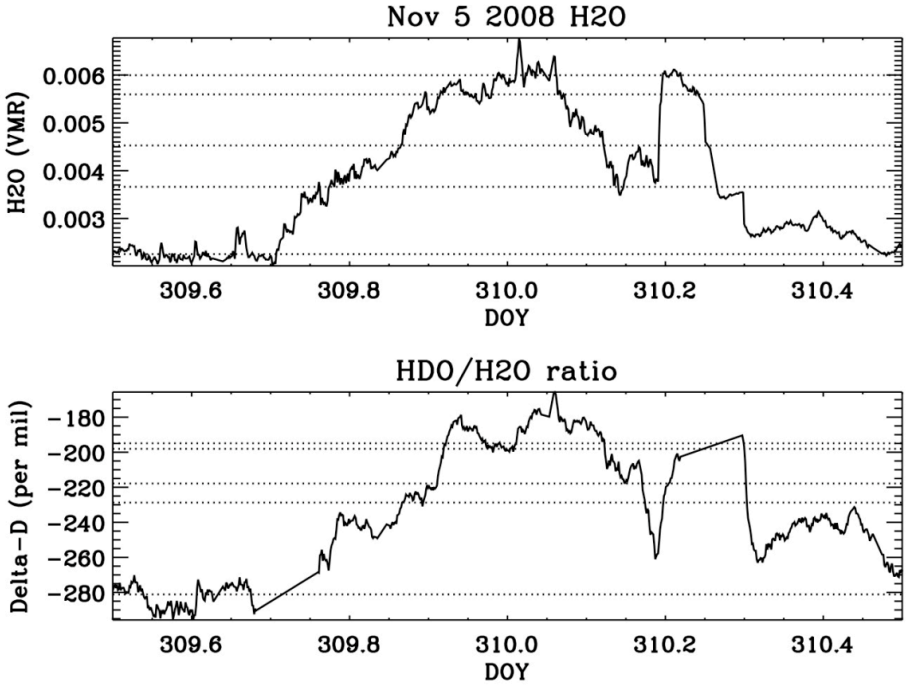

Fig. A6. Same as Fig. A2 but for 5 November 2008.

ACPD
10, 25355–25388, 2010

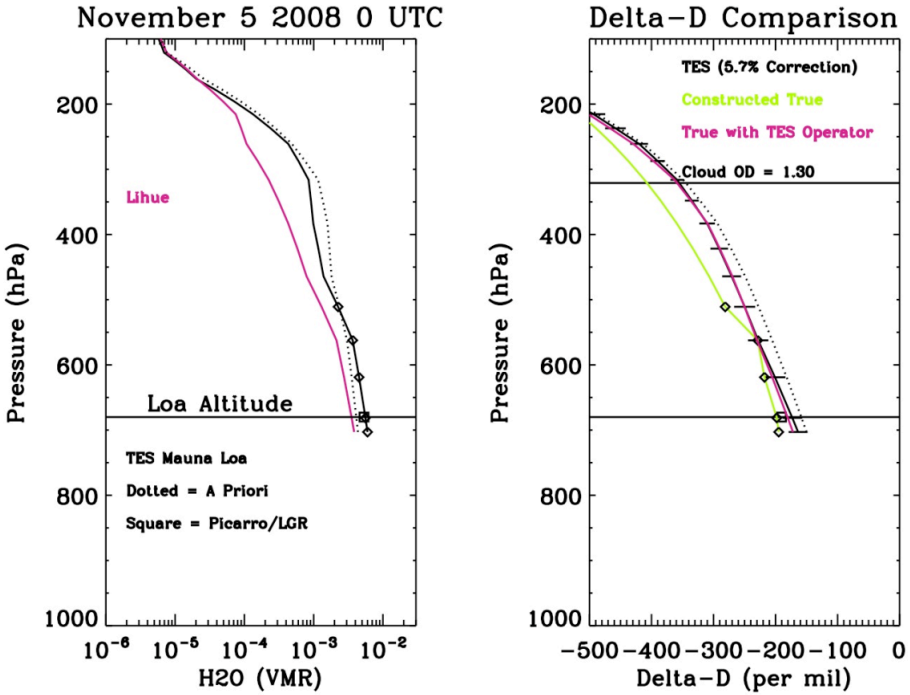

Fig. A7. Same as Fig. A3 but for 5 November 2008.

ACPD
10, 25355–25388, 2010

TES HDO/H_2O bias estimate

J. Worden et al.

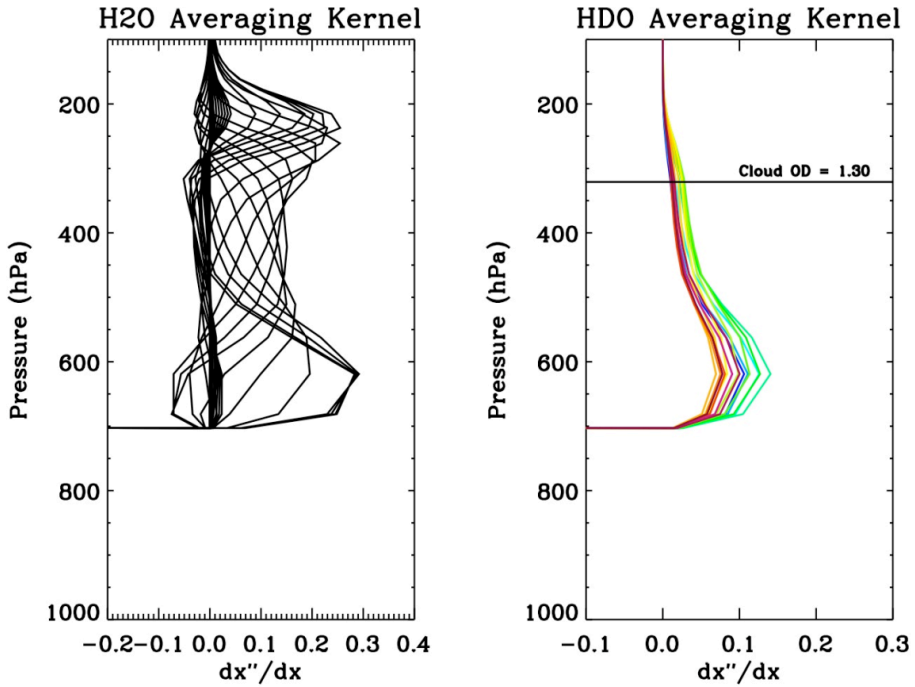

Fig. A8. Same as in Fig. A4 but for 5 November.

ACPD
10, 25355–25388, 2010